J. Cent. South Univ. (2012) 19: 3285−3290
DOI: 10.1007/s11771-012-1405-7

Springer

Dynamic−static coupling analysis on rockburst mechanism in jointed rock mass

JIA Peng(贾蓬), ZHU Wan-cheng(朱万成)

School of Resources and Civil Engineering, Northeastern University, Shenyang 110004, China

Abstract: A numerical code called RFPA-Dynamics was used to study the rockburst mechanism under dynamic load based on coupled static−dynamic analysis. The results show that dynamic disturbance has a very distinct triggering effect on rockburst. Under the dynamic load, rockburst is motivated by tensile stress formed by the overlapping of dynamic waves in the form of instantaneous open and cutting through of cracks in weak planes and pre-damaged areas. Meanwhile, the orientation of joint sets has an obvious leading effect on rockburst locations. Finally, a higher initial static stress state before dynamic loading can cause more pre-damaged area, thus leading to a larger rockburst scope.

Key words: rockburst; dynamic disturbance; numerical simulation; jointed rock mass

1 Introduction

Rockburst is one of the often encountered damages during underground excavation, which can not only cause construction delay and economic losses, but also can be a great threat to the safety of shift members.

Confusion may arise due to the wide-spread use of many different terms to describe a rockburst, including seismic event, pillar burst, crush burst, strain burst, and fault slip event. KAISER et al [1] gave the definition as: damage to an excavation that occurs in a sudden or violent manner and is associated with a seismic event. MULLER's definition [2] on rockburst is: an unpredictable failure phenomenon of sudden displace of surrounding rock mass caused by kinetic energy changing from the abrupt released elastic energy. Whereas, in Chinese coal mining industry, rockburst is often called as coal bumps [3], which refers to the instantaneous failure of coal seam accompanied by diffused coal powder due to drastic release of elastic energy. ORTLEEP and STACEY [4] indicated that the common characteristic of rockburst is the fierce ejection of rock from tunnel periphery.

Some researchers summarized the mechanism as three factors: intact hard rock, high tectonic stress and high ratio of redistributed stress to uniaxial compressive strength of rock mass [5−6]. But facts are not always like this. For example, during the excavation of horizontal inducer of Qinling Railway Tunnel II in China [7], intensive rockburst was encountered only at a depth of 60−100 m. On the contrary, in Lingxiadong tunnel section of Qinling railway tunnel with a depth of 1 700 m, the intensity of rockburst can only be classified as general, and the frequency as well as the intensity of rockburst did not increase with depth. During the excavation of Hongtoushan Copper Mine located in Liaoning Province of China with depth over 1 257 m, rockburst was encountered only at a depth of 400 m. The intensity of rockburst increased after depth of 700 m, but was fairly encountered after a depth of 1 077 m [8]. Another example is the construction of Norway Sima power plant tunnel. In the intensive rockburst area, the ratio of tangential stress to uniaxial compressive strength ($\sigma_\theta/\sigma_{uc}$) is only 0.2, which is too small for the traditional recognition of rockburst threshold [9]. According to LIU and XU [10], most of the rockbursts are located near to the excavation face instead of right in the excavation area, which means that rockbursts may not caused by the high value of the ratio, or else the rockburst events should only occur at the excavation site. WHYATT and BOARD [11] reported that 75% of rockbursts happened on blasting or several hours after blasting. Furthermore, under the same geological conditions, rockburst is more prone to be encountered by drill and blast method other than TBM tunnelling method [5, 10].

All the facts mentioned above are difficult to be explained by static theory unless the contribution of

Foundation item: Project(90401004) supported by the Fundamental Research Funds for the Central Universities of China; Projects(20100471465, 201104572) supported by China Postdoctoral Science Foundation; Project(20091029) supported by Postdoctoral Science Foundation of Liaoning Province, China; Projects(50934006, 51111130206) supported by the National Natural Science Foundation of China
Received date: 2011−10−25; **Accepted date:** 2012−01−13
Corresponding author: JIA Peng, Assistant Professor, PhD; Tel: +86−24−83687005; E-mail: jiapeng@mail.neu.edu.cn

dynamic disturbance on rockbursts is taken into account, which includes blasts, shake, stress changing due to the nearby rockburst, earthquake and so on [12−13].

Based on ORTLEPP's classification, KAISER et al [1] reduced the rockburst mechanism into three categories: buckling due to rock breakage, rock ejection due to earthquake energy transmission and rock fall due to earthquake. The first type of rockburst is self-initiated and the locations of rockburst and the seismic source are at the same place. However, the last two types of rockburst are caused by far field vibroseis. It is very important to diagnose the source mechanism of rockburst, so that the right support measurements can be adopted and the rockburst hazard can be avoided.

However, most of the studies on rockburst are aimed at the self-initiated rockburst, which is generally encountered in hard intact rock mass with high tectonic stress or high $\sigma_\theta/\sigma_{uc}$ value. The last two types of rockburst are seldom studied. In fact, most of the ejection and rock fall are encountered in jointed rock mass, where the far field dynamic disturbance is transformed into kinetic energy of the rock blocks cut by jointed sets. Based on this consideration, a numerical investigation on rockburst in jointed rock mass under dynamic load was conducted based on static−dynamic coupled method.

2 Mechanical behavior of jointed rock mass under static−dynamic load

2.1 Description of RFPA-Dynamics for coupled static−dynamic analysis

In RFPA-Dynamics, the solid or structure is assumed to be composed of many mesoscopic elements with the same size, whose material properties are different from one to another and are specified according to a Weibull distribution. Initially, an element is considered elastic, with elastic properties defined by elastic modulus and Poisson ratio. Damage is modeled by degrading the elastic modulus of the element for which the following damage criteria are satisfied at the element level:

$$F_1 \equiv \sigma_3 \equiv -f_{t0}, \quad F_2 \equiv \sigma_1 - \sigma_3 \frac{1+\sin\phi}{1-\sin\phi} \tag{1}$$

The first term of Eq. (1) is the simple tensile strength criterion whilst the latter one is the classical Mohr-Coulomb failure criterion. ZHAO [14] performed a series of dynamic uniaxial and triaxial compression, uniaxial tension and unconfined shear tests to examine the validity and applicability of the Mohr-Coulomb criterion. According to ZHAO's conclusion, the rock material strength under dynamic loads can be approximately described by the Mohr-Coulomb criterion. Thus, element may fail in either shear (corresponding to the Mohr-Coulomb failure criterion) or tensile status (corresponding to the tensile strength criterion). The sign convention used in this work is that compressive stress and strain are positive. Once Eq. (1) is satisfied at the element level, the elastic modulus of the element is reduced by the following formula:

$$E = (1-\omega)E_0 \tag{2}$$

where ω represents the damage variable, and E and E_0 are the elastic moduli of the damaged and undamaged elements, respectively. The element and its damage are assumed to be isotropic and elastic, therefore, E, E_0 and ω are all scalar quantities. In addition, the following relation between dynamic uniaxial compressive strength and loading rate, which has been proposed by ZHAO [14], is used to reflect the effect of stress rate on the dynamic strength:

$$f_{c0} = A(\dot{\sigma} / \dot{f}_{cs0}) + f_{cs0} \quad \text{when} \quad \dot{\sigma} > \dot{f}_{cs0} \tag{3}$$

where f_{c0} is the dynamic uniaxial compressive strength (MPa), $\dot{\sigma}$ is the stress rate (MPa/s), f_{cs0} is the uniaxial compressive strength at the quasi-static stress rate $\dot{f}_{cs0}$ that is approximately 5×10^{-2} MPa/s, and A is a material parameter. In addition, the experimental results of ZHAO [14] also indicated that the ratio of tensile to compressive strength and internal frictional angle are not influenced by the stress rate.

The numerical simulation on the dynamic disturbance induced failure of statically stressed rock includes two steps: The first step is the deformation and damage process analysis of rock (or rock mass) under static conditions, where the excavation induced stress redistribution around the underground opening can be captured. The second step is to carry out failure process analysis of pre-stressed rock triggered by dynamic disturbance. For more detailed descriptions about RFPA-Dynamics, as well as its validations for simulating the rock failure under static and dynamic loading, one can refer to Refs. [15−18].

2.2 Numerical model

The numerical model is 150 mm×150 mm in size and is composed of 150×150 iso-parametric elements (Fig. 1). The mean compressive strength of rock mass is 100 MPa and the mean elastic modulus is 60 GPa. The Poison ratio and internal frictional angle are 0.25 and 30°, respectively. A circular tunnel with a diameter of 26 mm is excavated in the middle of the model. Two sets of orthogonal joints are included in the model at a dip of 45° and 135°. The distance between joint sets is 7 mm. The mean compressive strength of joints is 30 MPa and the mean elastic modulus is 6 GPa. The Poison ratio and internal friction angle of joints are 0.4 and 20°, respectively.

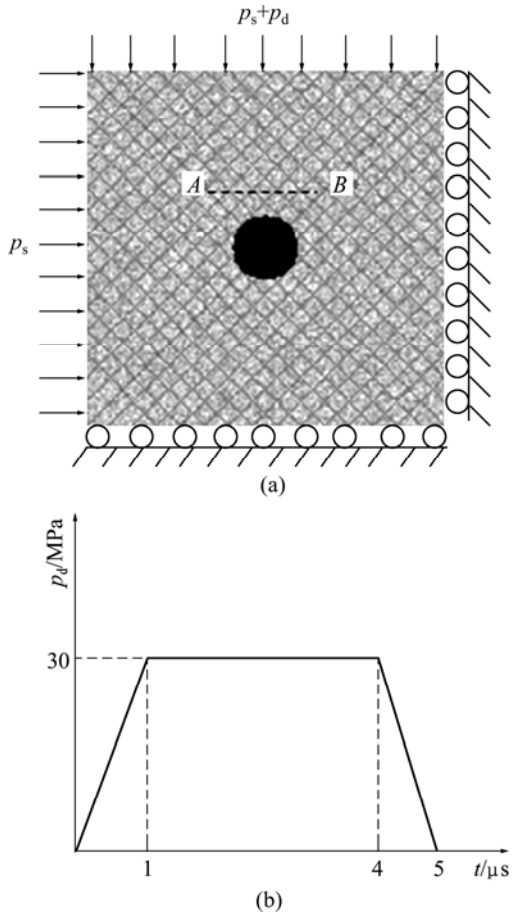

Fig. 1 Numerical model (a) and dynamic disturbance (b)

The model is simplified as a plane strain problem. Static stress is first applied on the left and top boundary of the model until it increases to a constant value, then a trapezoid dynamic disturbance is applied on the top boundary of model for 5 μs with amplitude of 30 MPa. In order to investigate the location and failure mode of rockburst, support is not taken into account.

2.3 Static−dynamic coupled analysis on rockburst in jointed rock mass

The top and horizontal stress load is increased gradually to 12.5 MPa with a constant lateral pressure coefficient of 1. Then, a dynamic load shown in Fig. 1 is applied on the top boundary of the model. At time t=0 μs (the vertical and horizontal stresses come to 12.5 MPa and no dynamic load is applied), local cracks and shear failure begin to initiate at the two sides of the arch crown (as shown in Fig. 2), where the rock mass is cut by the intersected joint sets. If the static stress load stops increasing, then the increase of local cracks will stop accordingly. This local failure is called self-initiated rockburst.

At time t=40 μs, cracks are connected rapidly due to the arriving of the dynamic stress wave (Fig. 2). This can be interpreted that due to the boundary effect of stress wave, part of the stress waves are reflected upon its arriving at tunnel boundary, and then superimposed with the coming stress waves into tensile waves thus leading to tensile failure in the weak joint planes above the arch crown. This can also be manifested by the changing curve of minimum principal stress versus time step of elements along *AB* line shown in Fig. 3 (the location of *AB* line is shown in Fig. 1).

At time t=45 μs, part of the minimum principal

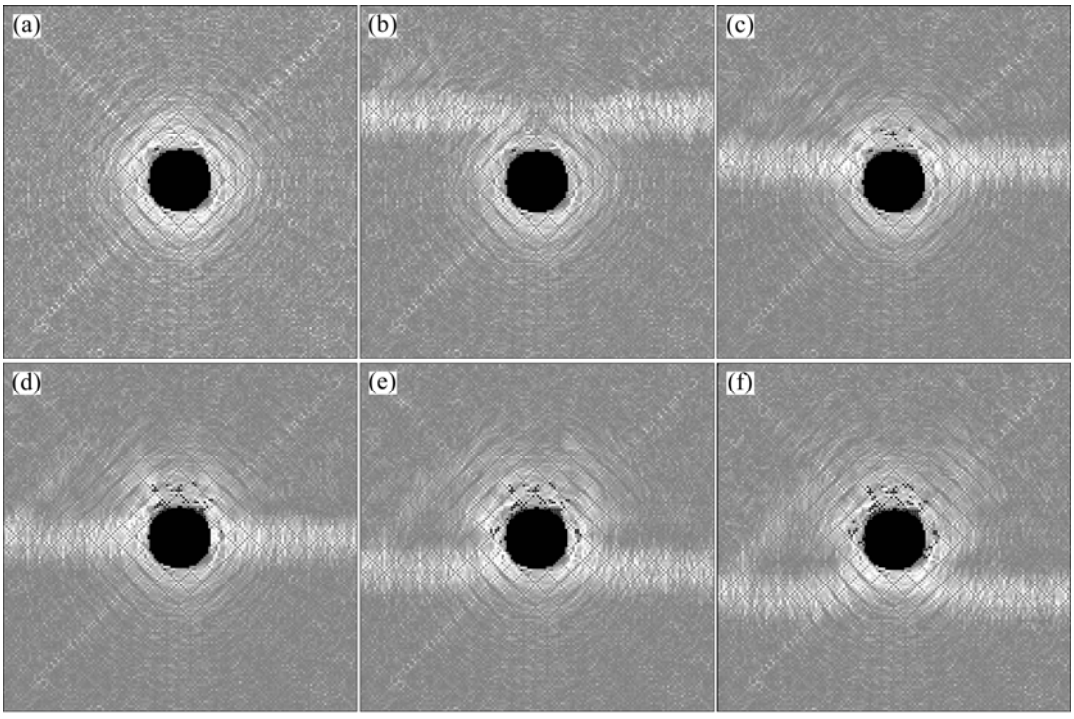

Fig. 2 Rockburst triggered dynamic disturbance: (a) t=0 μs; (b) t=30 μs; (c) t=40 μs; (d) t=45 μs; (e) t=50 μs; (f) t=55 μs

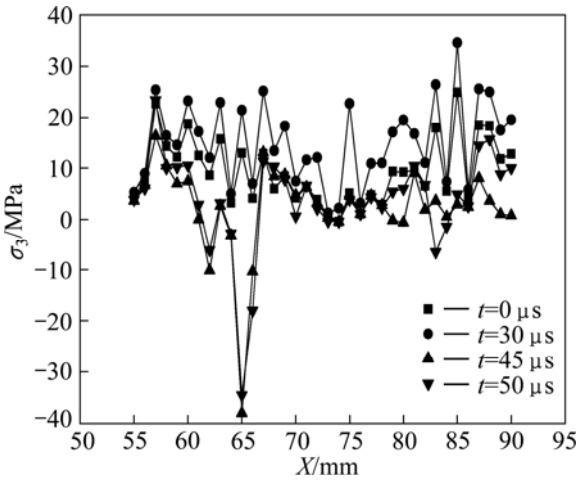

Fig. 3 Minimum principle stress along *AB* line

stress of elements along *AB* line has been converted into tensile stress, where tensile failure has been caused. With the downward transmission of stress waves, the range of crack opening and connection along joint planes increases so rapidly that rockburst is motivated with the formation of rock block falls. At this time, the scope of rockburst is larger than that under static loading conditions. Because the transmission direction of dynamic stress wave is from top to bottom of the model, the damage extent of rock mass above arch is far more extensive than elsewhere.

From numerical results, it can be concluded that dynamic disturbance has an important triggering effect on rockburst. Even the rock mass has already been in a balanced state, under dynamic disturbance, drastic increase of crack opening along the intersected joint planes can take place in the form of rockburst.

2.4 Correlation between joint orientations and rockburst locations

Generally, there are lots of joint sets existing in engineering rock mass, and it is rarely to see rock mass of one cubic meter containing no joints. These joint sets often occur and are more or less parallel to each other, or intersect with each other so that rock blocks are formed [19]. Due to the different characteristics of rock joints, such as orientation, mechanical property and connectivity of joint planes, the transmission of dynamic stress waves in jointed rock mass can be very complex.

In order to get some information on correlations between joint orientations and rockburst locations, two numerical models are built. Joint sets in Model 1 dip at angle of 0° and 90°. Joint sets in Model 2 dip at angle of 45° and 135°. Numerical simulation results are shown in Fig. 4.

The velocity of stress wave is different in two models due to the different orientations of joint set. Although the transmission velocity in Model 1 is much slower than in Model 2, its failure scope of rockburst is much larger. This is because the transmission direction of dynamic wave is in the same direction with the orientation of joint planes. The orientation of joint sets has a distinct leading effect on the locations of rockburst.

2.5 Effect of initial static stress state on rockburst scope under dynamic disturbance

In order to investigate the effect of dynamic disturbance on rockburst under different static loading conditions, two static stress states before dynamic loading are modeled. Hydro static load conditions of 12.5 MPa and 20 MPa are applied on the boundary of numerical model, respectively (Fig. 5), and the rockburst

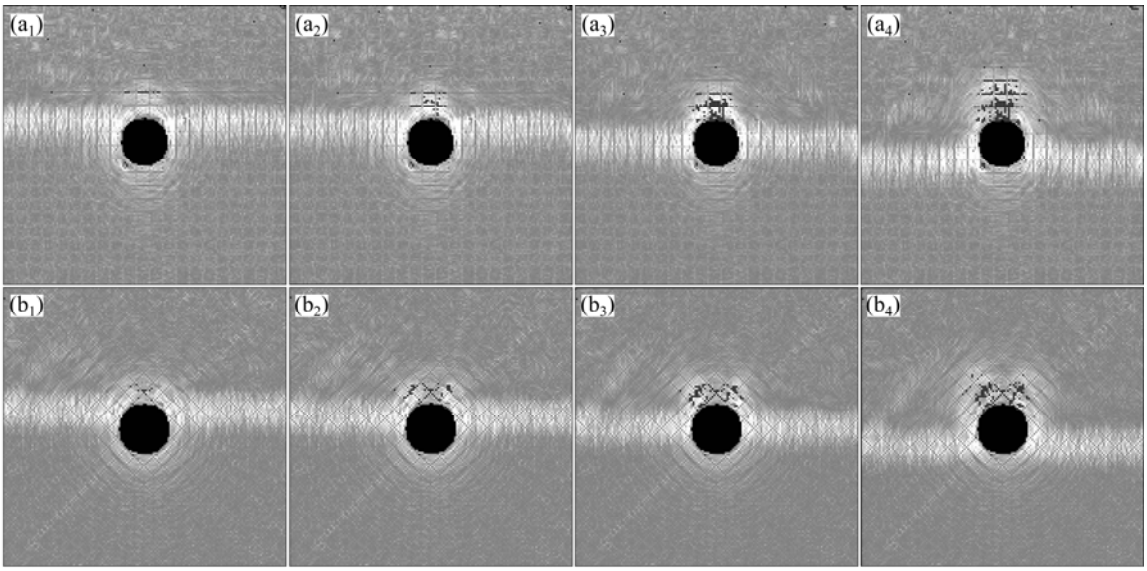

Fig. 4 Rockburst process and shear stress distribution under dynamic disturbance in models containing two joint sets with different dip angles: (a) Mode 1; (a_1) t=48 μs; (a_2) t=50 μs; (a_3) t=55 μs; (a_4) t=62 μs; (b) Mode 2; (b_1) t=38 μs; (b_2) t=40 μs; (b_3) t=43 μs; (b_4) t=48 μs

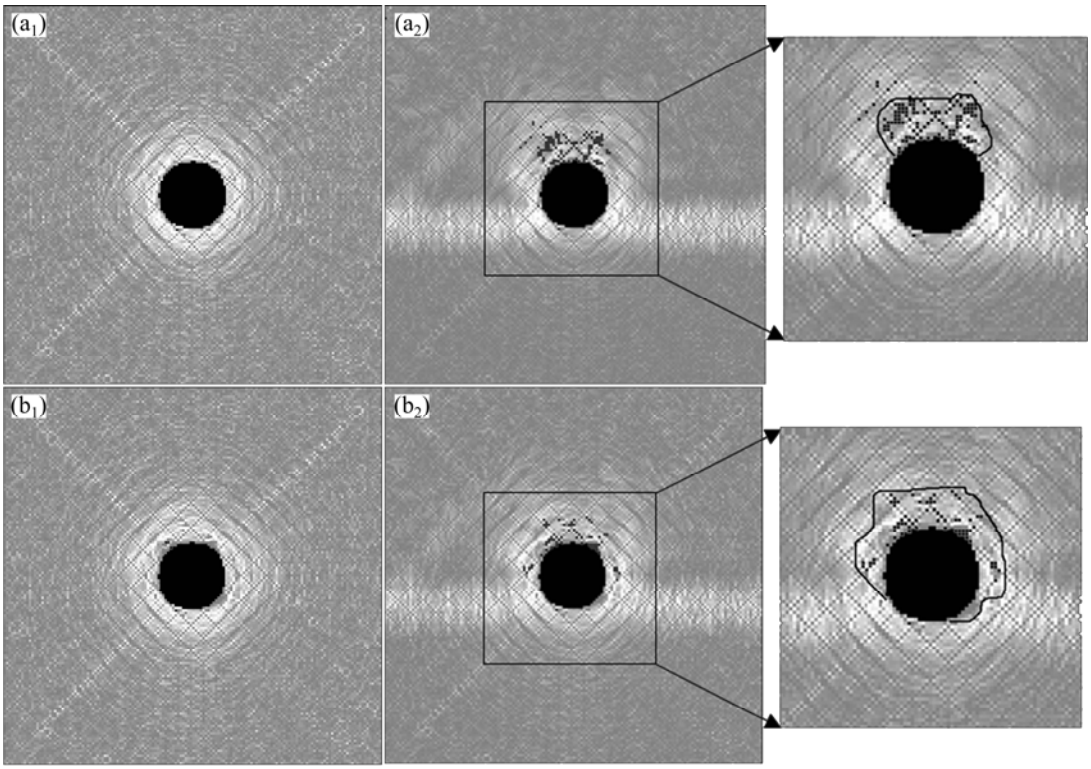

Fig. 5 Impact of joint orientations on rockburst scope under dynamic disturbance: (a_1) p_s=12.5 MPa, t=0 μs; (a_2) p_s=12.5 MPa, t=50 μs; (b_1) p_s=20.0 MPa, t=0 μs; (b_1) p_s=20.0 MPa, t=50 μs

scope after dynamic loading at time t=50 μs is compared.

At t=50 μs, the rockburst area for model under initial static stress of 12.5 MPa is mainly focused on the crown area, whereas for model under initial static stress of 20 MPa, the rockburst area is focused both on crown and sidewalls. The enlargement of rockburst scope is directly due to the increase of damage in weak joint surfaces under higher initial static stress state (or $\sigma_\theta/\sigma_{uc}$ ratio) before the application of dynamic stress wave. Once the dynamic disturbance is applied, the pre-damaged zones are more likely to move into tunnel, thus leading to a larger scope of rockburst.

3 Conclusions

1) A numerical code called RFPA-Dynamics is used to analyze the mechanism of rockburst in jointed rock mass based on static−dynamic coupled analysis. Numerical simulation results show that dynamic disturbance has a distinct triggering effect on rockburst in jointed rock mass. The sudden open and cutting through joint planes and other pre-existing weak zones by tensile stress wave formed by the boundary effect are the main mechanisms of rockburst in jointed rock mass. The orientation of joint sets has a leading effect on the location of rockburst areas. Rockburst scope under dynamic disturbance also depends on the initial static stress state of rock mass. A higher initial stress state can cause more damage area in rock mass before dynamic loading, thus can lead to a larger rockburst scope.

2) It should be noted that under dynamic disturbance, the occurrence of rockburst and its scope can be also affected by lateral pressure coefficient ratio, excavation method, mode of stress wave application, and so on, which should be taken into account in the future study.

References

[1] KAISER P K, McCREATH K R, TANNANT D D. Rockburst Research Handbook: A comprehensive summary of five years of collaborative research on rockbursting in hardrock mines [M]. Sudbury, Onfario: CAMIRO Mining Division, 1998: 3.

[2] MULLER W. Numerical simulation of rockbursts [J]. Mining Science and Technology, 1991, 12: 27−42.

[3] QI Qing-xin, CHEN Shang-ben, WANG Huai-xin, MAO De-bing, WANG Yong-xiu. Study on the relations among coal bump, rockburst and mining tremor with numerical simulation [J]. Chinese Journal of Rock Mechanics and Engineering, 2003, 22(11): 1852−1858. (in Chinese)

[4] ORTLEPP W D, STACEY T R. Rockburst mechanisms in tunnels and shafts [J]. Tunnelling and Underground Space Technology, 1994, 9(1): 59−65.

[5] ZHANG Zhi-qiang, GUAN Bao-shu, WENG Han-min. Basic analysis of rockbursting occurrence condition [J]. Journal of the China Railway Society, 1998, 20(4): 82−85. (in Chinese)

[6] RUDAJEV V, TEISSEVRE R, KOZAK J, SILENY J. Possible mechanism of rockbursts in coal mines [J]. Pure and Applied Geophysics, 1986, 124(4/5): 841−855.

[7] LI Chun-jie. The rockburst character and disposal during construction of Qinling tunnel [J]. World Tunnel, 1999(1): 36−41. (in Chinese)

[8] WANG Xu-zhao, WANG Hong-yong, QU Jin-hong. Characteristic of rockburst disaster and its geological conditions in the Hongtoushan copper mine [J]. Geology and Prospecting, 2005, 41(6): 102−106. (in Chinese)

[9] ANDERS C, TOMMY O. Rockbursting phenomena in a superficial rock mass in southern central Sweden [J]. Rock Mechanics and Rock Engineering, 1982, 15(2): 99−110.

[10] LIU Si-yu, XU Ze-min. Rockburst control of deeply buried tunnels based on coupling of dynamic and static stresses [J]. Journal of Natural Disasters, 2010, 19(1): 177−184. (in Chinese)

[11] WHYATT J K, BOARD M P. International Journal of Rock Mechanics and Mining Sciences & Geomechanics, 1991, 28(6): 341342.

[12] WANG Xian-neng, HUANG Run-qiu. Analysis of the influence of the dynamic disturbance on rockburst [J]. Mountain Research, 1998, 16(3): 188−192. (in Chinese)

[13] WANG J A, PARK H D. Comprehensive prediction of rockburst based on analysis of strain energy in rocks [J]. Tunnelling and Underground Space Technology, 2001, 16: 49−57.

[14] ZHAO J. Applicability of Mohr–Coulomb and Hoek–Brown strength criteria to the dynamic strength of brittle rock [J]. International Journal of Rock Mechanics and Mining Sciences, 2000, 37: 105−112.

[15] ZHU W C, TANG C A. Micromechanical model for simulating the fracture process of rock [J]. Rock Mechanics and Rock Engineering, 2004, 37(1): 25−56.

[16] ZHU W C, TANG C A. Numerical simulation of Brazilian disk rock failure under static and dynamic loading [J]. International Journal of Rock Mechanics and Mining Sciences, 2006, 43(2): 236−252.

[17] ZHU W C, LIU J, TANG C A, ZHAO X D, BRADY B H. Simulation of progressive fracturing processes around underground excavations under biaxial compression [J]. Tunnelling and Underground Space Technology, 2005, 20(3): 231−247.

[18] ZHU W C, LI Z H, ZHU L, TANG C A. Numerical simulation on rockburst of underground opening triggered by dynamic disturbance [J]. Tunnelling and Underground Space Technology, 2010, 25: 587−599.

[19] PRIEST, STEPHEN D. Discontinuity analysis for rock engineering [M]. London: Chapman & Hall, 1993: 17.

(Edited by YANG Bing)